

Enhancement of arsenic trioxide-induced apoptosis in HeLa cells by diethyldithiocarbamate or buthionine sulfoximine

YONG HWAN HAN, SUNG ZOO KIM, SUHN HEE KIM and WOO HYUN PARK

Department of Physiology, Medical School, Institute for Medical Sciences,
Chonbuk National University, JeonJu 561-180, Korea

Received January 24, 2008; Accepted March 27, 2008

Abstract. Arsenic trioxide (ATO) affects many biological functions such as cell proliferation, apoptosis, differentiation and angiogenesis in various cells. We investigated the *in vitro* effects of ATO as a reactive oxygen species (ROS) generator or a glutathione (GSH) depletor on apoptosis in HeLa cells. ATO decreased the viability of HeLa cells in a dose-dependent manner with an IC_{50} of approximately 5-6 μ M. ATO triggered apoptosis, which is accompanied by the loss of mitochondrial transmembrane potential ($\Delta\Psi_m$). Intracellular general ROS levels in HeLa cells were increased or decreased depending on the concentration of ATO. Particularly, the levels of $O_2^{\cdot-}$ were increased by ATO. In addition, we detected a decreased GSH content in ATO-treated cells. The GSH-depleted cells mainly showed propidium iodine-positive staining, indicating that the majority of the cells were dead. Diethyldithiocarbamate (DDC; an inhibitor of Cu,Zn-SOD) induced apoptosis and the loss of mitochondrial transmembrane potential ($\Delta\Psi_m$) in HeLa control cells. DDC intensified apoptosis, the loss of mitochondrial transmembrane potential, increased levels of $O_2^{\cdot-}$ and GSH depletion in ATO-treated cells. L-buthionine sulfoximine (BSO; an inhibitor of GSH synthesis) did not induce apoptosis in HeLa control cells, but

increased levels of apoptosis, $O_2^{\cdot-}$ and GSH depletion in ATO-treated cells. In conclusion, the changes in intracellular GSH levels rather than ROS levels are tightly related to the enhancement of ATO-induced apoptosis in HeLa cells by DDC or BSO.

Introduction

Arsenic trioxide (ATO; As_2O_3) was initially reported to induce complete remission in patients with relapsed or refractory acute promyelocytic leukemia (APL) without severe marrow suppression (1). The antiproliferative effect of ATO is not limited to APL cells, but can also be observed in a variety of hematological malignancies (2,3). Accumulating evidence indicates that ATO regulates many biological functions such as cell proliferation, apoptosis, differentiation and angiogenesis in various cell lines such as renal (4), head and neck (5), ovarian (6), prostate (6) and gastric (7) cancer cells. ATO as a mitochondrial toxin induces a loss of mitochondrial transmembrane potential (2,4) and, as such, it induces the generation of reactive oxygen species (ROS) (8,9). These phenomena trigger the apoptosis of target cells. Therefore, it is thought that ATO induces apoptosis in tumor cells by affecting the mitochondria and ROS generation. In addition, it has been reported that the intracellular GSH content has a decisive effect on ATO-induced apoptosis (10,11). Furthermore, a combination of ATO and L-buthionine sulfoximine (BSO; an inhibitor of GSH synthesis) induced synergistic cytotoxicity in several cell lines of renal cell carcinoma (10), leukemia (11) and other solid tumors (12).

ROS include hydrogen peroxide (H_2O_2), the superoxide anion ($O_2^{\cdot-}$) and the hydroxyl radical ($\cdot OH$). These molecules were recently implicated in the regulation of many important cellular events, including transcription factor activation, gene expression, differentiation and cellular proliferation (13). ROS are formed as by-products of mitochondrial respiration or oxidases, including nicotine adenine diphosphate (NADPH) oxidase, xanthine oxidase (XO), and certain arachidonic acid oxygenases (14). A change in the redox state of the tissue implies a change in ROS generation or metabolism. Principal metabolic pathways include superoxide dismutase (SOD), which is expressed as extracellular, intracellular, and mitochondrial isoforms. These isoforms metabolize $O_2^{\cdot-}$ to H_2O_2 . Further metabolism by peroxidases that include catalase and glutathione peroxidase yields O_2 and H_2O (15). Cells

Correspondence to: Dr Woo Hyun Park, Department of Physiology, Medical School, Chonbuk National University, JeonJu 561-180, Korea
E-mail: parkwh71@chonbuk.ac.kr

Abbreviations: ATO, arsenic trioxide; ROS, reactive oxygen species; NADPH, nicotine adenine diphosphate; XO, xanthine oxidase; SOD, superoxide dismutase; APL, acute promyelocytic leukemia; FBS, fetal bovine serum; MTT, 3-(4,5-dimethylthiazol-2-yl)-2,5-diphenyltetrazolium bromide; PI, propidium iodine; PBS, phosphate-buffered saline; FITC, fluorescein isothiocyanate; DAPI, 4'-6-diamidino-2-phenylindole; H_2DCFDA , 2',7'-dichlorodihydrofluorescein diacetate; DHE, dihydroethidium; GSH, glutathione; CMFDA, 5-chloromethylfluorescein diacetate; DDC, diethyldithiocarbamate; BSO, L-buthionine sulfoximine

Key words: arsenic trioxide, reactive oxygen species, apoptosis, HeLa, glutathione, diethyldithiocarbamate, L-buthionine sulfoximine

possess antioxidant systems to control the redox state, which is important for their survival. Excessive production of ROS gives rise to the activation of events that lead to death or survival in several cell types (16,17). The exact mechanisms involved in cell death induced by ROS are not fully understood, and the protective effect mediated by some antioxidants remains controversial.

Diethyldithiocarbamate (DDC) is a metal ion-chelating and thiol-containing agent which is a well-known inhibitor of Cu,Zn-SOD by ligation and removal of Cu(II) ions from its active site (18). DDC has also been described as an inhibitor of nuclear factor (NF κ B) and is able to trap nitric oxide (NO) (19,20). These activities result in an increase in superoxide production in cells and tissues. Glutathione (GSH) is a main non-protein antioxidant in the cell and it clears away the superoxide anion free radical and provides electrons for enzymes such as glutathione peroxidase, which reduce H₂O₂ to H₂O. GSH has been shown to be crucial for the regulation of cell proliferation, cell cycle progression and apoptosis (21,22) and is known to protect cells from toxic insult through detoxification of toxic metabolites of drugs and ROS (23). For instance, in rat cerebral astrocytes, DDC-induced cytotoxicity was ameliorated by incubation with GSH (24). Conversely, DDC was not affected by changes in the GSH status in rat hippocampal astrocytes (25).

In the present study, we evaluated the *in vitro* effects of ATO on the viability of HeLa cells in relation to apoptosis, investigated its mechanism in relation to ROS and GSH levels, and examined the effects of DDC and BSO on ATO-treated HeLa cells.

Materials and methods

Cell culture. Human cervical adenocarcinoma HeLa cells were maintained in humidified incubator containing 5% CO₂ at 37°C. HeLa cells were cultured in DMEM supplemented with 10% fetal bovine serum (FBS) and 1% penicillin-streptomycin (Gibco BRL, Grand Island, NY). Cells were routinely grown in 100-mm plastic tissue culture dishes (Nunc, Roskilde, Denmark) and harvested with a solution of trypsin-EDTA while in a logarithmic phase of growth. Cells were maintained in these culture conditions for all experiments.

Reagents. ATO, DDC and BSO were purchased from Sigma-Aldrich Chemical Co. (St. Louis, MO). ATO was dissolved in 1.65 M NaOH at 1x10⁻¹ M as a stock solution. DDC, BSO and AT were dissolved in distilled water at 1x10⁻¹ M as a stock solution. The stock solutions were wrapped in foil and kept at 40 or -20°C.

Cell viability assay. The *in vitro* cell viability effect of ATO on HeLa cells was determined by measuring the 3-(4,5-dimethylthiazol-2-yl)-2,5-diphenyltetrazolium bromide (MTT) dye absorbance as described previously (2). In brief, cells (2x10⁵ cells/well) were seeded in 96-well microtiter plates in the presence of the designated doses of ATO with or without DDC, BSO or AT (Nunc). After exposure to the drug for 72 h, 50 μ l of MTT (Sigma) solution (2 mg/ml in PBS) was added to each well, and the plates were incubated for an additional 3 or 4 h at 37°C. MTT solution in medium was

removed following centrifugation of the plates. To achieve solubilization of the formazan crystals formed in viable cells, 100 or 200 μ l of DMSO was added to each well. The optical density of each well was measured at 570 nm using a microplate reader (Spectra Max 340, Molecular Devices Co., Sunnyvale, CA, USA). Each plate contained multiple wells at a given experimental condition and multiple control wells. This procedure was replicated for 2-4 plates/condition.

Sub-G₁ analysis. The sub-G₁ cell population was determined by staining DNA with propidium iodide (PI; Sigma) as previously described (26). PI is a fluorescent biomolecule that can be used to stain DNA (Ex/Em = 488 nm/617 nm). In brief, 1x10⁶ cells were incubated with the designated doses of ATO for 72 h. Cells were then washed in phosphate-buffered saline (PBS) and fixed in 70% ethanol. Cells were again washed with PBS and then incubated with PI (10 μ g/ml) with simultaneous treatment of RNase at 37°C for 30 min. The percentages of cells having the sub-G₁ DNA content were measured with a FACStar flow cytometer (Becton Dickinson, San Jose, CA) and analyzed using Lysis II and Cellfit software (Becton Dickinson) or ModFit software (Verity Software Inc.).

Annexin V/PI staining. Apoptosis was determined by staining cells with annexin V-fluorescein isothiocyanate (FITC) (Ex/Em = 495 nm/529 nm) and PI labeling, since annexin V can be used to identify the externalization of phosphatidylserine during the progression of apoptosis and, therefore, can detect cells during the early phase of apoptosis. PI can also be used to differentiate necrotic, apoptotic and normal cells. This agent is membrane impermeant and generally excluded from viable cells. In brief, 1x10⁶ cells were incubated with the designated doses of ATO with or without DDC, BSO or AT for 72 h. Cells were washed twice with cold PBS and then resuspended in 500 μ l of binding buffer (10 mM HEPES/NaOH pH 7.4, 140 mM NaCl, 2.5 mM CaCl₂) at a concentration of 1x10⁶ cells/ml. Annexin V-FITC (5 μ l) (Pharmingen, San Diego, CA) and PI (1 μ g/ml) were then added to the cells, which were analyzed with a FACStar flow cytometer. Viable cells were negative for both PI and annexin V; apoptotic cells were positive for annexin V and negative for PI, whereas late apoptotic or necrotic cells displayed both high annexin V and PI labeling. Non-viable cells, undergoing necrosis, were positive for PI and negative for annexin V.

Measurement of mitochondrial membrane potential ($\Delta\Psi_m$). The mitochondrial membrane was monitored using the Rhodamine 123 fluorescent dye (Ex/Em = 507 nm/529 nm), a cell-permeable cationic dye, which preferentially enters the mitochondria based on the highly negative mitochondrial membrane potential ($\Delta\Psi_m$). Depolarization of mitochondrial membrane potential ($\Delta\Psi_m$) results in the loss of Rhodamine 123 from the mitochondria and a decrease in intracellular fluorescence. In brief, 1x10⁶ cells were incubated with the designated doses of ATO with or without DDC, BSO or AT for 72 h. Cells were washed twice with PBS and incubated with Rhodamine 123 (0.1 μ g/ml; Sigma) at 37°C for 30 min. PI (1 μ g/ml) was subsequently added, and Rhodamine 123 and PI staining intensity were determined by flow cytometry.

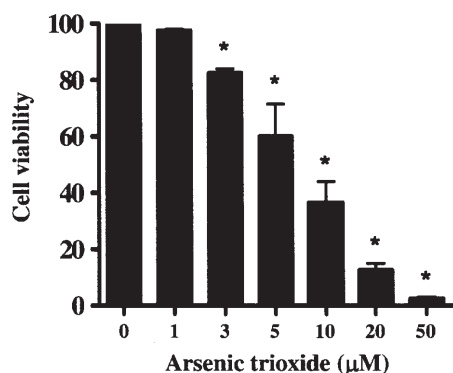


Figure 1. Effects of ATO on the viability of HeLa cells *in vitro*. Exponentially growing cells were treated with the indicated concentrations of ATO for 72 h. Cell viability was assessed by MTT assays. Results represent the mean of at least three independent experiments. Bars, SD (standard deviation of the mean); *P<0.05 compared with the ATO-untreated control group.

Detection of intracellular general ROS and $O_2^{\cdot-}$ concentration. Intracellular general ROS such as H_2O_2 , $\cdot OH$ and $ONOO\cdot$ were detected by means of an oxidation-sensitive fluorescent probe dye, 2',7'-dichlorodihydrofluorescein diacetate (H_2DCFDA) (Invitrogen Molecular Probes, Eugene, OR). H_2DCFDA was deacetylated intracellularly by nonspecific esterase, which was further oxidized by cellular peroxides, yielding 2,7-dichlorofluorescein (DCF), a fluorescent compound (Ex/Em = 495 nm/529 nm). DCF is poorly selective for the superoxide anion radical ($O_2^{\cdot-}$). In contrast, dihydroethidium (DHE) (Ex/Em = 518 nm/605 nm) (Invitrogen Molecular Probes) is a fluorogenic probe that is highly selective for $O_2^{\cdot-}$ among ROS. DHE is cell-permeable and reacts with the superoxide anion to form ethidium, which in turn is intercalated in deoxyribonucleic acid, thereby exhibiting a red fluorescence. In brief, cells were incubated with the designated doses of ATO with or without DDC, BSO or AT for 72 h. Cells were then washed in PBS and incubated with 20 μM H_2DCFDA or 5 μM DHE at 37°C for 30 min according to the manufacturer's instructions. DCF fluorescence and red fluorescence were detected using a FACStar flow cytometer. For each sample, 5,000 or 10,000 events were collected. ROS and $O_2^{\cdot-}$ levels were expressed as the mean fluorescence intensity (MFI), which was calculated by CellQuest software.

Detection of intracellular glutathione (GSH). Cellular GSH levels were analyzed using 5-chloromethylfluorescein diacetate (CMFDA, Molecular Probes). CMFDA is a useful membrane-permeable dye (Ex/Em = 492 nm/517 nm) for determining levels of intracellular glutathione as previously described (27). In brief, cells were incubated with the designated doses of ATO with or without DDC, BSO or AT for 72 h. Cells were then washed with PBS and incubated with 5 μM CMFDA at 37°C for 30 min according to the manufacturer's instructions. Cytoplasmic esterases convert nonfluorescent CMFDA to fluorescent 5-chloromethylfluorescein, which can then react with GSH. PI (1 $\mu g/ml$) was subsequently added, and CMF fluorescence and PI staining

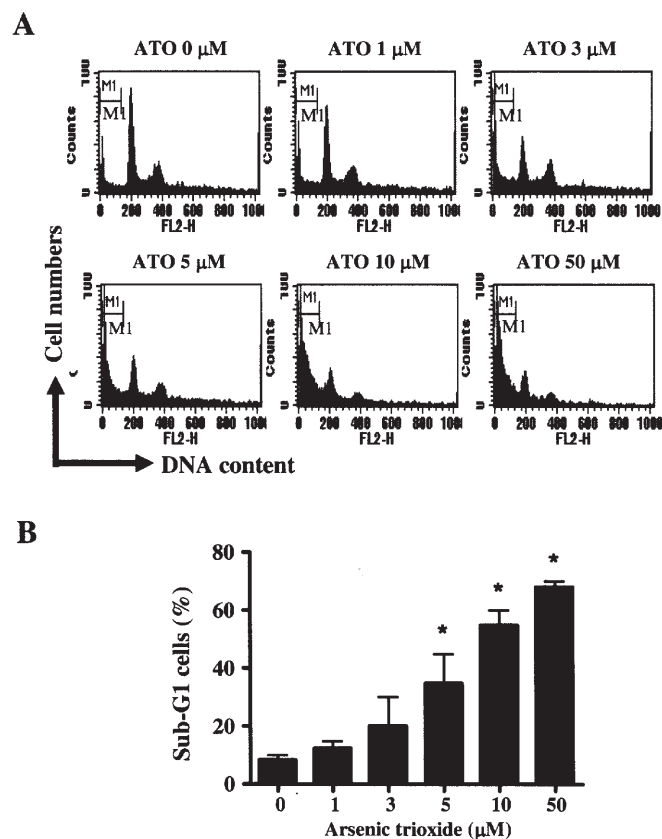


Figure 2. Effects of ATO on the sub-G₁ population of HeLa cells. Exponentially growing cells were treated with the indicated concentrations of ATO for 72 h. (A) Sub-G₁ cells were counted by DNA flow cytometric analysis. The M1 region of the histogram indicates the sub-G₁ population of the HeLa cells. (B) The graph shows the percentages of sub-G₁ in A. *P<0.05 compared with the ATO-untreated control group. Bar, SD of the mean.

intensity were determined using a FACStar flow cytometer and calculated by CellQuest software. For each sample, 5,000 or 10,000 events were collected.

Statistical analysis. Results represent the mean of at least three independent experiments. Microsoft Excel or Instat software (GraphPad Prism4, San Diego, CA) was used to analyze the data. The Student's t-test or one-way analysis of variance (ANOVA) with post hoc analysis using the Tukey's multiple comparison test was used for parametric data. Statistical significance was defined as p<0.05.

Results

Effects of ATO on the viability of HeLa cells. We examined the effect of ATO on the viability of HeLa cells using an MTT assay. A dose-dependent decrease in cell viability was observed in HeLa cells with an IC₅₀ of ~5-6 μM ATO at 72 h (Fig. 1). We performed an *in vitro* apoptosis detection assay to determine whether ATO induced apoptosis in HeLa cells. As shown in Fig. 2A and B, ATO increased the sub-G₁ population in a dose-dependent manner at 72 h. Following exposure to 5 μM ATO, the percentage of HeLa cells in sub-G₁ phase was ~33%. To characterize the cell death induced

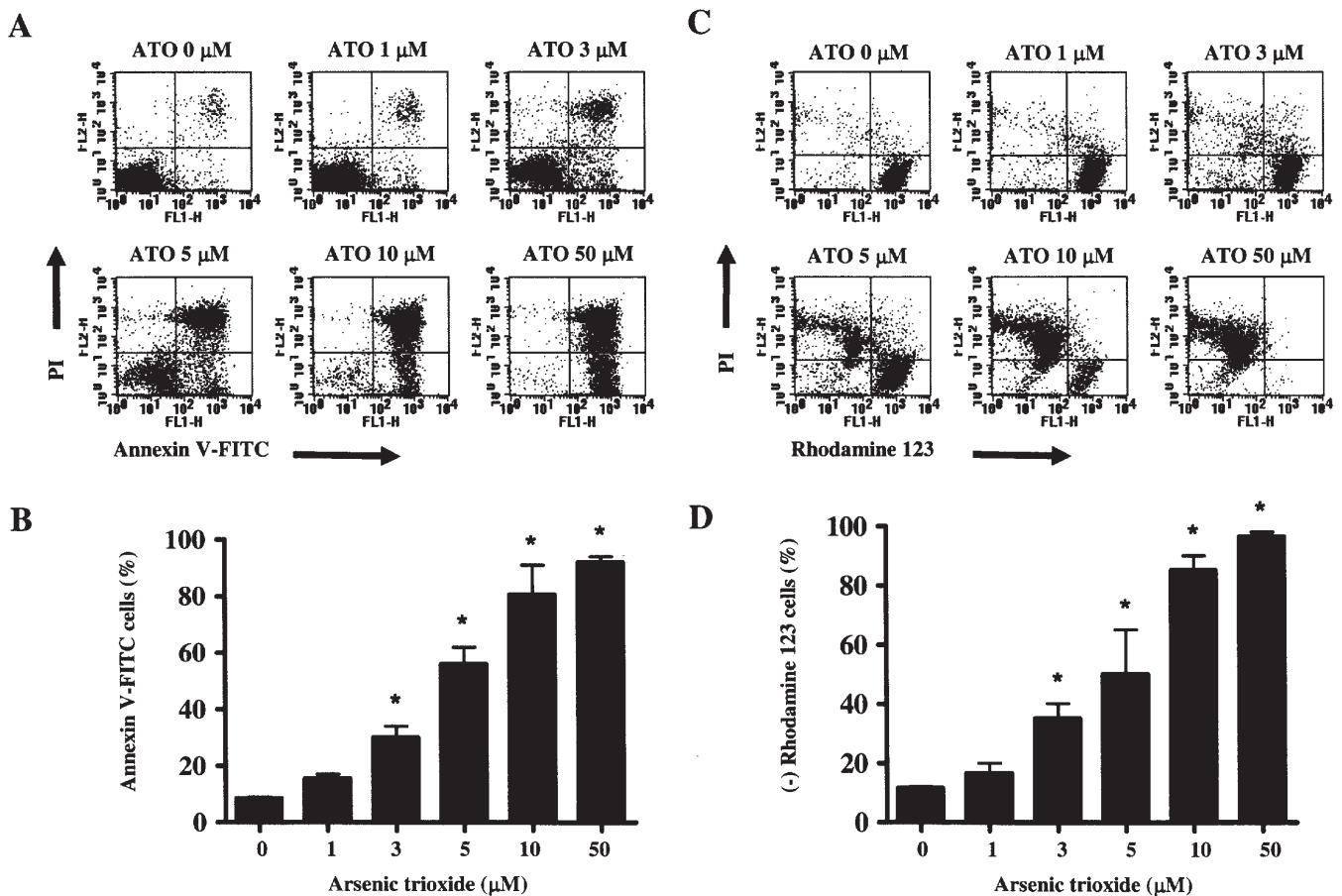


Figure 3. Effects of ATO on the plasma membrane and mitochondrial transmembrane potential ($\Delta\Psi_m$) in HeLa cells. Exponentially growing cells were treated with the indicated concentrations of ATO for 72 h. (A) Cells with annexin V staining were counted with a FACStar flow cytometer. (B) The graph shows the percentage of annexin V-positive cells in A. (C) Cells stained with Rhodamine 123 were counted with a FACStar flow cytometer. (D) The graph shows the percentage of Rhodamine 123-negative cells in C. * $P < 0.05$ as compared with the ATO-untreated control group. Bar, SD of the mean.

by ATO, we examined the nuclear morphologies of dying cells using the fluorescent DNA-binding agent, DAPI. HeLa cells, treated with 5 or 10 μM of ATO for 72 h, displayed typical morphological features of apoptotic cells, i.e., condensed nuclei (data not shown).

Effects of ATO on the plasma membrane and mitochondrial transmembrane potential ($\Delta\Psi_m$) in HeLa cells. To further confirm and evaluate the induction of apoptosis, we stained cells with annexin V and PI. Similar to the percentage of the sub- G_1 cells, the proportion of annexin V-staining cells in the ATO-treated cells increased in a dose-dependent manner (Fig. 3A and B). We also detected a small number of necrotic HeLa cells (annexin V-negative and PI-positive cells). Next, we attempted to elucidate the effect of ATO on the mitochondrial membrane potential ($\Delta\Psi_m$) using the Rhodamine 123 dye. The proportion of Rhodamine 123 negative-staining cells was very similar to that of the annexin V-positive cells by ATO (Fig. 3C and D). Following exposure to 5 μM ATO, the percentage of Rhodamine 123-negative cells was ~46%, indicating that ATO efficiently triggered the loss of mitochondrial membrane potential ($\Delta\Psi_m$).

Effects of ATO on ROS and GSH production in HeLa cells. To assess the production of intracellular ROS in ATO-treated

HeLa cells, we used H_2DCFDA fluorescent dye. As shown in Fig. 4A and D, intracellular general ROS levels were increased in HeLa cells treated with the lower concentrations of ATO (1 and 3 μM) for 72 h. However, the relatively higher concentrations of ATO (5, 10 or 50 μM) reduced the intracellular ROS levels. When we treated HeLa cells with ATO for short time periods (1 or 2 h), we observed decreased levels of ROS in these cells (data not shown). Treatment with 10 μM ATO reduced the ROS levels more than those with treatment with 1 μM ATO. Next, we attempted to detect the change in intracellular $\text{O}_2^{\cdot-}$ in ATO-treated HeLa cells. Red fluorescence derived from DHE reflecting $\text{O}_2^{\cdot-}$ accumulation was increased in ATO-treated HeLa cells (Fig. 4B and E). However, treatment with ATO slightly decreased intracellular $\text{O}_2^{\cdot-}$ levels in HeLa cells for short time periods of 1 h (data not shown). We analyzed the GSH levels in HeLa cells using CMF fluorescence. The M1 population of HeLa cells (Fig. 4C) showed lower levels of intracellular GSH content. ATO significantly elevated the percentage of cells in the M1 phase at 72 h in a dose-dependent manner (Fig. 4C and F), which indicated the depletion of intracellular GSH content in ATO-treated HeLa cells. To evaluate whether or not the M1 cells in the negative CMF fluorescence region were dead, we additionally stained the cells with PI to verify the disruption of the plasma membrane. As shown in Fig. 5A and B, the

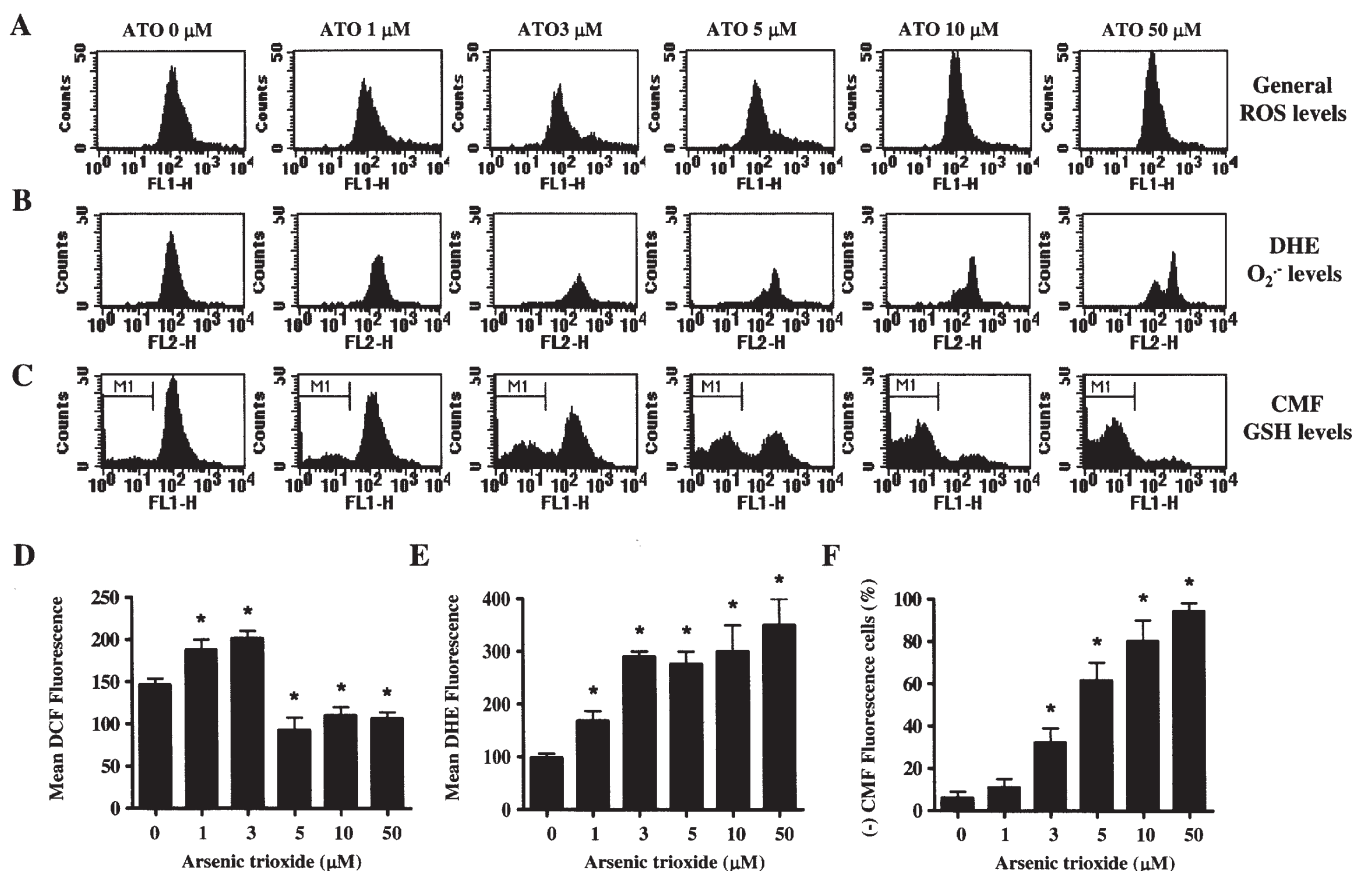


Figure 4. Effects of ATO on ROS and GSH levels in HeLa cells. Exponentially growing cells were treated with the indicated concentrations of ATO for 72 h. Intracellular general ROS levels (A), intracellular $O_2^{\bullet-}$ levels (B) and intracellular GSH levels (C) were determined by a FACStar flow cytometer as described in Materials and methods. The graphs show the levels of mean DCF fluorescence in A (D) and the mean DHE fluorescence in B (E) and the percent of CMF-negative fluorescent cells (GSH-depleted cells) in C (F). * $P < 0.05$ as compared with the ATO-untreated control group. Bar, SD of the mean.

negative CMF fluorescent cells mainly showed PI-positive staining in a dose-dependent manner, indicating that the cells undergoing GSH depletion were predominantly dead. The negative CMF fluorescence and PI-negative cells were still observed at the lower doses of 3 and 5 μM ATO treatment, indicating that the cells treated with the lower concentration of ATO strongly preserved the integrity of the cell membrane in CMF-negative cells (Fig. 5A and C). When HeLa cells were treated with ATO for short time periods (1 or 2 h), we observed that ATO decreased the GSH levels (mean CMF fluorescence) in HeLa cells in a dose-dependent manner (data not shown).

Effects of DDC and BSO on ROS and GSH production in ATO-treated HeLa cells. We investigated whether DDC (a well-known inhibitor of Cu,Zn-SOD) and BSO (an inhibitor of GSH synthesis) altered the ROS and GSH content in ATO-treated cells at 72 h. Treatment with 1 μM DDC decreased the intracellular ROS levels in 5 μM ATO-treated HeLa cells and control cells (Fig. 6A). Treatment with 1 μM BSO increased the intracellular ROS levels in 1 or 5 μM ATO-treated HeLa cells (Fig. 6A). DDC increased the intracellular $O_2^{\bullet-}$ levels in 5 μM ATO-treated HeLa cells and control cells (Fig. 6B). Treatment with BSO increased the intracellular $O_2^{\bullet-}$ levels in 1 or 5 μM ATO-treated HeLa cells (Fig. 6B). Treatment with DDC increased the depletion of the

GSH content (negative CMF fluorescence) in 5 μM ATO-treated HeLa cells or control cells (Fig. 6C). BSO increased the depletion of the GSH content in 1 or 5 μM ATO-treated HeLa cells while this agent did not significantly deplete the GSH content in HeLa control cells (Fig. 6C). In addition, as shown in Fig. 7, the percentage of CMF-negative and PI-positive fluorescent cells (36.6%) was increased in 1 μM DDC-treated HeLa cells, as compared with that of HeLa control cells (3.1%). The proportion of CMF-negative and PI-positive cells (75.9%) was markedly increased by treatment with ATO and DDC, which indicated that DDC exaggerated the disruption of the plasma membrane of ATO-treated cells. In contrast, the percentage of CMF-positive and PI-positive cells was <5% in HeLa cells treated with ATO and/or DDC or without both (Fig. 7), indicating that the majority of cells in the CMF-positive region were alive.

Effects of DDC and BSO on ATO-induced apoptosis in HeLa cells. Next, we investigated the effects of DDC and BSO on ATO-induced HeLa cell death. Treatment with DDC slightly reduced the viability of ATO-treated or -untreated cells (Fig. 8A). BSO intensified ATO-induced HeLa cell death while this agent did not influence the viability of HeLa control cells (Fig. 8A). Treatment with DDC alone increased the number of annexin V-positive cells in HeLa control cells, and DDC exaggerated the number of annexin V-positive

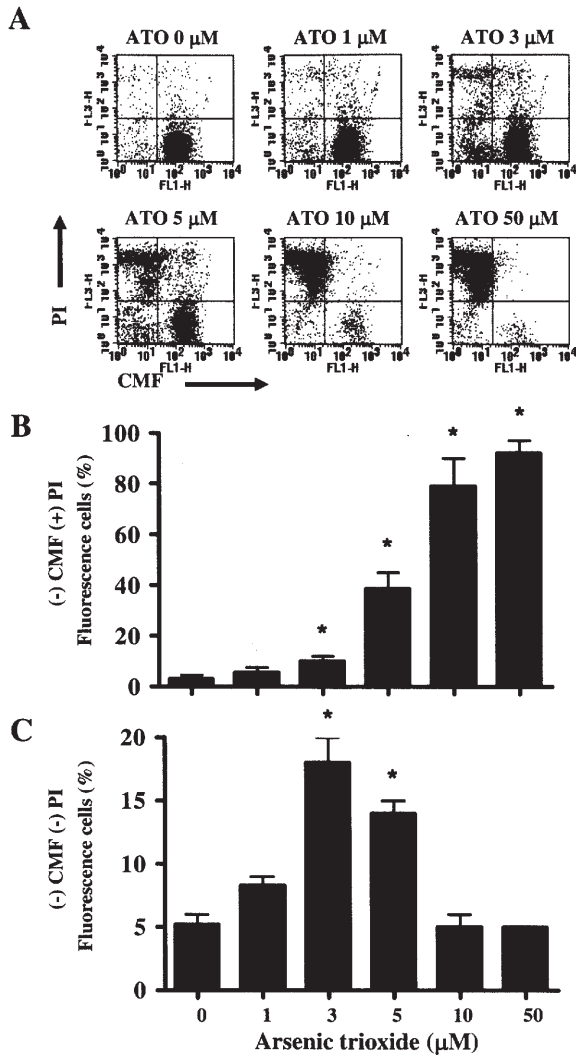


Figure 5. Effects of ATO on CMF (GSH content) and PI (plasma membrane integrity) fluorescence in HeLa cells. Exponentially growing cells were treated with the indicated concentrations of ATO for 72 h. (A) CMF fluorescent cells and PI-staining cells were measured with a FACStar flow cytometer. (B) The graph shows the percentage of CMF-negative and PI-positive-staining cells in A. (C) The graph shows the percentage of CMF-negative- and PI-negative-staining cells in A. *P<0.05 as compared with the ATO-untreated control group. Bar, SD of the mean.

cells in 5 μM ATO-treated HeLa cells (Fig. 8B). BSO increased annexin V-positive cells in ATO-treated HeLa cells while this agent did not increase annexin V-positive cells in HeLa control cells (Fig. 8B). Concerning the mitochondrial membrane potential, treatment with DDC intensified the loss of mitochondrial transmembrane potential ($\Delta\Psi_m$) in 5 μM ATO-treated HeLa cells (Fig. 8C). DDC alone induced the loss of mitochondrial transmembrane potential ($\Delta\Psi_m$) as well (Fig. 8C). BSO intensified the loss of mitochondrial transmembrane potential ($\Delta\Psi_m$) in ATO-treated cells while this agent did not influence the loss of mitochondrial transmembrane potential ($\Delta\Psi_m$) in HeLa control cells (Fig. 8C).

Discussion

We focused on the effects of ATO in relation to ROS and GSH on the viability of HeLa cells. We also examined the effects of DDC (a SOD inhibitor) and BSO (a GSH synthesis inhibitor) on ATO-treated HeLa cells. Our data showed that ATO potently induced apoptosis in a dose-dependent manner in HeLa cells. It has been suggested that a high ratio of Bax to Bcl-2 causes the collapse of the mitochondrial membrane potential ($\Delta\Psi_m$), resulting in release of cytochrome c and apoptosis (28). To ascertain whether ATO induces the loss of mitochondrial membrane potential ($\Delta\Psi_m$), we used Rhodamine 123, a cell-permeable cationic dye for measuring mitochondrial membrane potential ($\Delta\Psi_m$). According to our data, ATO induced the loss of mitochondrial membrane potential ($\Delta\Psi_m$) in a dose-dependent manner in HeLa cells. These results confirm that ATO primarily damages the mitochondria of target cells which stimulates progression to the next step of apoptosis.

ATO can disturb the natural oxidation and reduction equilibrium in cells, leading to an increase in ROS by a variety of redox enzymes, including flavoprotein-dependent superoxide-producing enzymes such as NADPH oxidase (8,9,29). ATO decreases glutathione (GSH) and increases the intracellular ROS level in certain APL cells (11). Therefore, to elucidate the involvement of ROS in ATO-induced HeLa cell death, we assessed the ROS levels using H₂DCFDA and

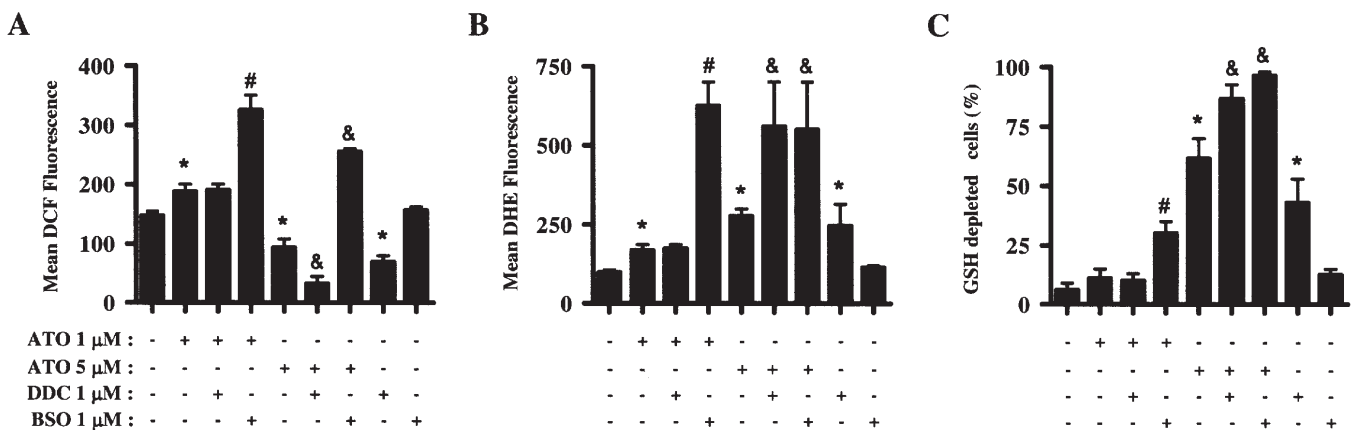


Figure 6. Effects of DDC and BSO on the intracellular ROS and GSH production in ATO-treated HeLa cells. Exponentially growing cells were treated with 1 or 5 μM ATO and/or 1 μM DDC or 1 μM BSO for 72 h. (A) Intracellular general ROS levels. (B) Intracellular O₂[•] levels. (C) The percentages of GSH-depleted cells. *P<0.05 as compared with the ATO-untreated control group; #P<0.05 as compared with the 1 μM ATO-treated group; &P<0.05 as compared with the 5 μM ATO-treated group. Bar, SD of the mean.

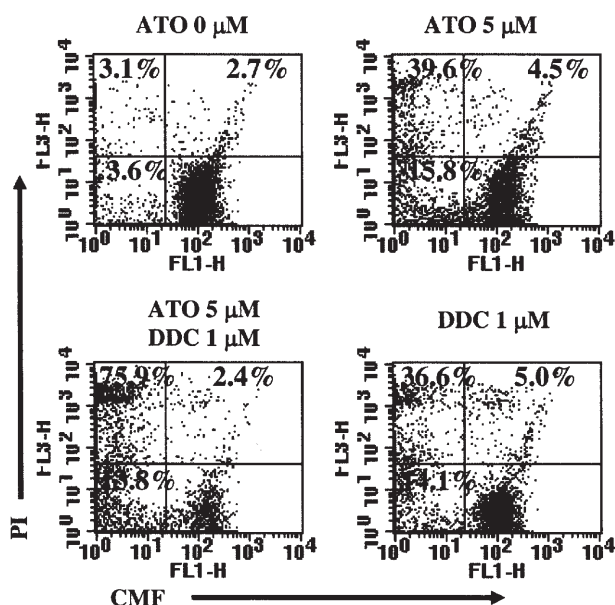


Figure 7. Effects of DDC on CMF and PI fluorescence in ATO-treated HeLa cells. Exponentially growing cells were treated with 5 μM ATO and/or 1 μM DDC for 72 h. CMF fluorescent cells and PI-staining cells were counted with a FACStar flow cytometer. The percentage of CMF-negative- and PI-positive-staining cells (upper left quadrant), CMF-negative- and PI-negative-staining cells (lower left quadrant), CMF-positive- and PI-positive-staining cells (upper right quadrant) are indicated for each figure.

DHE fluorescence. Our data showed that the intracellular ROS level was increased in HeLa cells treated with lower doses of ATO (1 or 3 μM) at 72 h. This result is consistent with other reports, showing that increased intracellular ROS such as H_2O_2 levels play an important role in ATO-induced cell death in cervical cancer cells (30), APL cells (31), hepatocellular carcinoma HepG2 (32) and glioblastoma A172 cells (33). In fact, Woo *et al* reported that ATO induced apoptosis through a ROS-dependent pathway in HeLa cells (34). However, this study did not determine the intracellular

H_2O_2 level in HeLa cells treated with ATO doses $>5 \mu\text{M}$ and even showed that the H_2O_2 levels in 2 μM ATO-treated HeLa cells were higher than those in 3 μM ATO-treated HeLa cells at 30 h. Similarly, our current results showed that higher doses of ATO ($>5 \mu\text{M}$) inducing apoptosis efficiently in HeLa cells did not increase intracellular ROS levels at 72 h. We recently demonstrated that 7 μM ATO induced apoptosis along with a decrease in intracellular ROS levels in As4.1 juxtglomerular cells (35). In addition, treatment with ATO (1-10 μM) decreased intracellular ROS levels in HeLa cells at early time points (1 or 2 h). These results suggest the possibility that ATO has biphasic effects on ROS levels depending on the concentration of this agent and incubation times. It is also possible that higher doses of ATO or the first priming exposure to ATO directly inhibits nonspecific esterases which deacetylates H_2DCFDA , resulting in the reduced production of 2,7-dichlorofluorescein (DCF). Haga *et al* found that H_2O_2 accumulation was detected in ATO-treated glioblastoma T98G cells, but apoptosis did not occur in these cells (33). DDC, giving rise to intensified apoptotic effects on 5 μM ATO-treated HeLa cells, decreased the ROS levels further. BSO increased the levels of apoptosis accompanied with an augmentation of ROS levels in ATO-treated cells. These results suggest that the apoptotic effects of ATO are not tightly related to intracellular ROS levels.

Next, we attempted to investigate whether or not another ROS, $\text{O}_2^{\cdot-}$, was increased by ATO. ATO accumulated the content of $\text{O}_2^{\cdot-}$ in HeLa cells. It is possible that ATO directly or indirectly inhibited SOD, resulting in increased $\text{O}_2^{\cdot-}$ in HeLa cells. We observed that treatment with DDC increased the levels of $\text{O}_2^{\cdot-}$ and induced apoptosis in HeLa control cells, and also intensified those in 5 μM ATO-treated cells. However, DDC did not intensify the levels of $\text{O}_2^{\cdot-}$ and apoptosis in 1 μM ATO-treated cells. These data indicate that an increase in $\text{O}_2^{\cdot-}$ by DDC and its pro-apoptotic effects depend on the concentration of ATO in HeLa cells. In addition, we observed that treatment with 10 or 100 μM DDC did not increase the levels of $\text{O}_2^{\cdot-}$ and induce apoptosis in HeLa

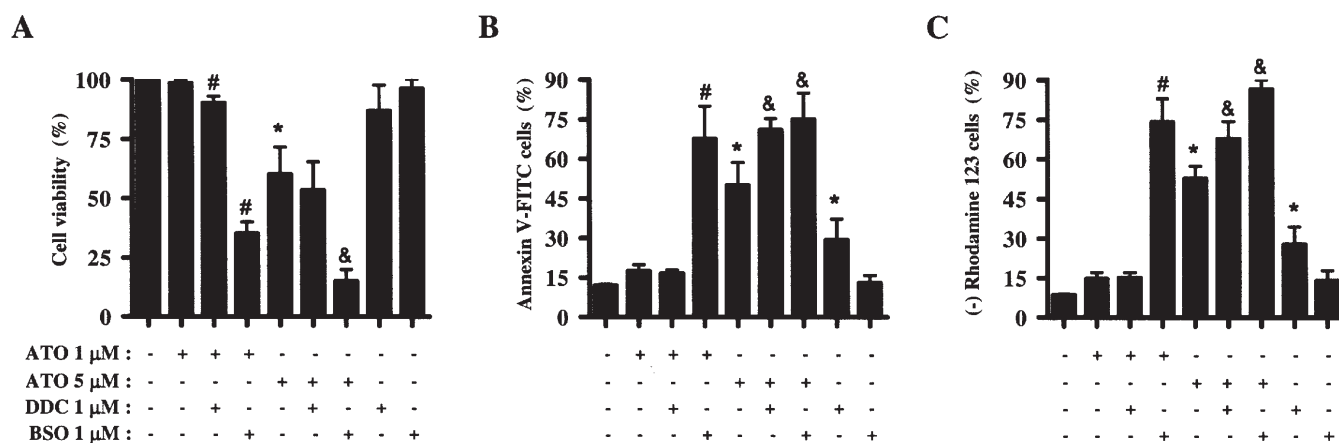


Figure 8. Effects of DDC and BSO on apoptosis in ATO-treated HeLa cells. Exponentially growing cells were treated with 1 or 5 μM ATO and/or 1 μM DDC or 1 μM BSO for 72 h. (A) Cell viability was assessed by MTT assays. Annexin V staining cells (B) and Rhodamine 123-negative-staining cells (C) were counted with a FACStar flow cytometer. * $P < 0.05$ as compared with the ATO-untreated control group; # $P < 0.05$ as compared with the 1 μM ATO-treated group; & $P < 0.05$ as compared with the 5 μM ATO-treated group. Bar, SD of the mean.

control cells (data not shown). Recently, Dumay *et al* showed that DDC exerts both pro- and anti-apoptotic functions on HeLa cells; ROS-dependent and -independent, respectively (36). Thus, it is possible that the pro-apoptotic effect of DDC can be inhibited or favored depending on its own concentration or its combination with other agents. Treatment with BSO significantly increased the intracellular $O_2^{\bullet-}$ levels in 1 or 5 μ M ATO-treated HeLa cells. BSO strongly intensified the reduced viability of ATO-treated cells while this agent did not influence the viability of HeLa control cells. These data suggest that an increase in $O_2^{\bullet-}$ levels is in part related to apoptosis in ATO-treated HeLa cells. The increased pattern of $O_2^{\bullet-}$ by ATO was reported in esophageal cancer SHEE85 cells (37), but this pattern was not observed in ATO-treated acute myelogenous leukemia HL-60 cells (38) and renal cell carcinoma ACHN cells (10). In addition, we did not find that ATO increased $O_2^{\bullet-}$ levels in HeLa cell at early time points (1 or 2 h). These discrepancies may be due to cell type specificity and different times or methods used to detect $O_2^{\bullet-}$ levels. Taken together, although the ROS changes by ATO are very important mediators in the induction of apoptosis in target cancer cells, the precise role of ROS in relation to this drug must be defined more clearly.

Intracellular GSH is a main non-protein antioxidant in the cell, and it clears away the superoxide anion free radical and provides electrons for enzymes such as glutathione peroxidase, which reduce H_2O_2 to H_2O . It has been reported that the intracellular GSH content has a decisive effect on ATO-induced apoptosis (10,11,32). Likewise, the depletion of intracellular GSH content was observed in ATO-induced apoptosis in HeLa cells at 72 h. In addition, we observed that ATO decreased GSH levels (mean CMF fluorescence) in HeLa cells in a dose-dependent manner at early time points. This finding suggests that ATO plays a role as a GSH depletor itself in HeLa cells. Treatment with DDC amplified the levels of GSH depletion and apoptosis in 5 μ M ATO-treated HeLa cells. The depleted GSH effect of DDC also depended on the concentration of ATO in HeLa cells. As expected, BSO increased the depletion of the GSH content and apoptosis in 1 or 5 μ M ATO-treated HeLa cells. Interestingly, treatment with neither 1 μ M BSO nor 1 μ M ATO significantly depleted the GSH content in HeLa control cells. Since ATO is known to react with thiols such as GSH in aqueous solution at a neutral pH (39), it is possible that 1 μ M BSO strongly induced GSH deletion in ATO-treated HeLa cells, which consequently resulted in apoptosis. These results suggest that intracellular GSH levels are tightly related to ATO-induced cell death. In addition, we observed that many of the negative CMF fluorescent cells showed PI-positive staining, indicating that the majority of cells showing GSH depletion were dead.

In summary, we demonstrated that ATO potently generates the production of $O_2^{\bullet-}$ and induces the depletion of the GSH content in HeLa cells. Treatment with DDC or BSO increased $O_2^{\bullet-}$ levels, GSH depletion and apoptosis levels in ATO-treated HeLa cells. In conclusion, the changes in intracellular GSH levels rather than ROS levels are tightly related to the enhancement of ATO-induced apoptosis in HeLa cells by DDC or BSO.

Acknowledgements

This research was supported by the Korean Research Foundation Grant funded by the Korean Government (MOEHRD, Basic Research Promotion Fund) (KRF-2007-331-E00018).

References

1. Soignet SL, Maslak P, Wang ZG, *et al.*: Complete remission after treatment of acute promyelocytic leukemia with arsenic trioxide. *N Engl J Med* 339: 1341-1348, 1998.
2. Park WH, Seol JG, Kim ES, *et al.*: Arsenic trioxide-mediated growth inhibition in MC/CAR myeloma cells via cell cycle arrest in association with induction of cyclin-dependent kinase inhibitor, p21, and apoptosis. *Cancer Res* 60: 3065-3071, 2000.
3. Zhang W, Ohnishi K, Shigeno K, *et al.*: The induction of apoptosis and cell cycle arrest by arsenic trioxide in lymphoid neoplasms. *Leukemia* 12: 1383-1391, 1998.
4. Hyun Park W, Hee Cho Y, Won Jung C, *et al.*: Arsenic trioxide inhibits the growth of A498 renal cell carcinoma cells via cell cycle arrest or apoptosis. *Biochem Biophys Res Commun* 300: 230-235, 2003.
5. Seol JG, Park WH, Kim ES, *et al.*: Effect of arsenic trioxide on cell cycle arrest in head and neck cancer cell line PCI-1. *Biochem Biophys Res Commun* 265: 400-404, 1999.
6. Uslu R, Sanli UA, Sezgin C, *et al.*: Arsenic trioxide-mediated cytotoxicity and apoptosis in prostate and ovarian carcinoma cell lines. *Clin Cancer Res* 6: 4957-4964, 2000.
7. Zhang TC, Cao EH, Li JF, Ma W and Qin JF: Induction of apoptosis and inhibition of human gastric cancer MGC-803 cell growth by arsenic trioxide. *Eur J Cancer* 35: 1258-1263, 1999.
8. Kim HR, Kim EJ, Yang SH, *et al.*: Combination treatment with arsenic trioxide and sulindac augments their apoptotic potential in lung cancer cells through activation of caspase cascade and mitochondrial dysfunction. *Int J Oncol* 28: 1401-1408, 2006.
9. Miller WH Jr, Schipper HM, Lee JS, Singer J and Waxman S: Mechanisms of action of arsenic trioxide. *Cancer Res* 62: 3893-3903, 2002.
10. Wu XX, Ogawa O and Kakehi Y: Enhancement of arsenic trioxide-induced apoptosis in renal cell carcinoma cells by L-buthionine sulfoximine. *Int J Oncol* 24: 1489-1497, 2004.
11. Dai J, Weinberg RS, Waxman S and Jing Y: Malignant cells can be sensitized to undergo growth inhibition and apoptosis by arsenic trioxide through modulation of the glutathione redox system. *Blood* 93: 268-277, 1999.
12. Maeda H, Hori S, Ohizumi H, *et al.*: Effective treatment of advanced solid tumors by the combination of arsenic trioxide and L-buthionine-sulfoximine. *Cell Death Differ* 11: 737-746, 2004.
13. Baran CP, Zeigler MM, Tridandapani S and Marsh CB: The role of ROS and RNS in regulating life and death of blood monocytes. *Curr Pharm Des* 10: 855-866, 2004.
14. Zorov DB, Juhaszova M and Sollott SJ: Mitochondrial ROS-induced ROS release: An update and review. *Biochim Biophys Acta* 1757: 509-517, 2006.
15. Wilcox CS: Reactive oxygen species: roles in blood pressure and kidney function. *Curr Hypertens Rep* 4: 160-166, 2002.
16. Chen TJ, Jeng JY, Lin CW, Wu CY and Chen YC: Quercetin inhibition of ROS-dependent and -independent apoptosis in rat glioma C6 cells. *Toxicology* 223: 113-126, 2006.
17. Simon HU, Haj-Yehia A and Levi-Schaffer F: Role of reactive oxygen species (ROS) in apoptosis induction. *Apoptosis* 5: 415-418, 2000.
18. Cocco D, Calabrese L, Rigo A, Argese E and Rotilio G: Re-examination of the reaction of diethyldithiocarbamate with the copper of superoxide dismutase. *J Biol Chem* 256: 8983-8986, 1981.
19. Schreck R, Meier B, Mannel DN, Droge W and Baeuerle PA: Dithiocarbamates as potent inhibitors of nuclear factor kappa B activation in intact cells. *J Exp Med* 175: 1181-1194, 1992.
20. James PE, Liu KJ and Swartz HM: Direct detection of tissue nitric oxide in septic mice. *Adv Exp Med Biol* 454: 181-187, 1998.
21. Poot M, Teubert H, Rabinovitch PS and Kavanagh TJ: De novo synthesis of glutathione is required for both entry into and progression through the cell cycle. *J Cell Physiol* 163: 555-560, 1995.

22. Schnelldorfer T, Gansauge S, Gansauge F, Schlosser S, Beger HG and Nussler AK: Glutathione depletion causes cell growth inhibition and enhanced apoptosis in pancreatic cancer cells. *Cancer* 89: 1440-1447, 2000.
23. Lauterburg BH: Analgesics and glutathione. *Am J Ther* 9: 225-233, 2002.
24. Trombetta LD, Toulon M and Jamall IS: Protective effects of glutathione on diethylthiocarbamate (DDC) cytotoxicity: a possible mechanism. *Toxicol Appl Pharmacol* 93: 154-164, 1988.
25. Hardej D and Trombetta LD: The effects of ebselen on cisplatin and diethylthiocarbamate (DDC) cytotoxicity in rat hippocampal astrocytes. *Toxicol Lett* 131: 215-226, 2002.
26. Park WH, Jung CW, Park JO, *et al*: Trichostatin inhibits the growth of ACHN renal cell carcinoma cells via cell cycle arrest in association with p27, or apoptosis. *Int J Oncol* 22: 1129-1134, 2003.
27. Han YH, Kim SH, Kim SZ and Park WH: Intracellular GSH levels rather than ROS levels are tightly related to AMA-induced HeLa cell death. *Chem Biol Interact* 171: 67-78, 2008.
28. Yang J, Liu X, Bhalla K, *et al*: Prevention of apoptosis by Bcl-2: release of cytochrome c from mitochondria blocked. *Science* 275: 1129-1132, 1997.
29. Chou WC, Jie C, Kenedy AA, Jones RJ, Trush MA and Dang CV: Role of NADPH oxidase in arsenic-induced reactive oxygen species formation and cytotoxicity in myeloid leukemia cells. *Proc Natl Acad Sci USA* 101: 4578-4583, 2004.
30. Kang YH, Yi MJ, Kim MJ, *et al*: Caspase-independent cell death by arsenic trioxide in human cervical cancer cells: reactive oxygen species-mediated poly(ADP-ribose) polymerase-1 activation signals apoptosis-inducing factor release from mitochondria. *Cancer Res* 64: 8960-8967, 2004.
31. Jing Y, Dai J, Chalmers-Redman RM, Tatton WG and Waxman S: Arsenic trioxide selectively induces acute promyelocytic leukemia cell apoptosis via a hydrogen peroxide-dependent pathway. *Blood* 94: 2102-2111, 1999.
32. Li JJ, Tang Q, Li Y, *et al*: Role of oxidative stress in the apoptosis of hepatocellular carcinoma induced by combination of arsenic trioxide and ascorbic acid. *Acta Pharmacol Sin* 27: 1078-1084, 2006.
33. Haga N, Fujita N and Tsuruo T: Involvement of mitochondrial aggregation in arsenic trioxide (As₂O₃)-induced apoptosis in human glioblastoma cells. *Cancer Sci* 96: 825-833, 2005.
34. Woo SH, Park IC, Park MJ, *et al*: Arsenic trioxide induces apoptosis through a reactive oxygen species-dependent pathway and loss of mitochondrial membrane potential in HeLa cells. *Int J Oncol* 21: 57-63, 2002.
35. Han YH, Kim SZ, Kim SH and Park WH: Arsenic trioxide inhibits growth of As4.1 juxtaglomerular cells via cell cycle arrest and caspase-independent apoptosis. *Am J Physiol Renal Physiol* 293: F511-F520, 2007.
36. Dumay A, Rincheval V, Trotot P, Mignotte B and Vayssiere JL: The superoxide dismutase inhibitor diethylthiocarbamate has antagonistic effects on apoptosis by triggering both cytochrome c release and caspase inhibition. *Free Radic Biol Med* 40: 1377-1390, 2006.
37. Shen ZY, Shen WY, Chen MH, Shen J and Zeng Y: Reactive oxygen species and antioxidants in apoptosis of esophageal cancer cells induced by As₂O₃. *Int J Mol Med* 11: 479-484, 2003.
38. Han SS, Kim K, Hahm ER, *et al*: Arsenic trioxide represses constitutive activation of NF-kappaB and COX-2 expression in human acute myeloid leukemia, HL-60. *J Cell Biochem* 94: 695-707, 2005.
39. Scott N, Hatlelid KM, MacKenzie NE and Carter DE: Reactions of arsenic(III) and arsenic(V) species with glutathione. *Chem Res Toxicol* 6: 102-106, 1993.